Cavitation-erosion resistance of three zinc-aluminum alloy for bearing application

a cura di: L. Montesano, A. Pola, G. M La Vecchia

L. Montesano, A. Pola, G. M La Vecchia
Dipartimento di Ingegneria Meccanica e Industriale,
Università degli Studi di Brescia

Zinc alloys are known as good competitors of copper alloys for some tribological applications, in both lubricated and dry conditions. In presence of lubricant, cavitation erosion phenomenon can occur, increasing the damaging of the part. In this paper a comparative study of the erosion resistance of an innovative (ZnAl15Cu1Mg) and two commercial Zn-Al alloys (ZA27 and Alzen305) is presented. Cavitation erosion tests were executed according to ASTM G32 on cast samples and the response of each material was assessed by measuring the worn volume as a function of cavitation time and by analyzing the damaged surfaces by means of optical and scanning electron microscope. It was pointed out that the new ZnAl15Cu1Mg guarantees better resistance than the traditional ZA27 and Alzen305 as a consequence of the different microstructure.

INTRODUCTION

Many zinc aluminum alloys are known for their good tribological behavior [1-5], low cost and ease production by foundry techniques [6-7]. As a function of the chemical composition, zinc alloys can exploit good wear resistance and assure lower friction coefficient than copper alloys [8].

In the last 30 years, different zinc alloys have been proposed as alternative material to bronze and brasses for the production of bearing and bushing, when high loads and low sliding speeds are applied [1, 8]. These components usually work dipped in lubricant. In this condition, variations of the applied load due to the rotation can cause pressure variations in the fluid, generating cavitation and thus erosive wear. This phenomenon increases the wear damaging related to rolling and sliding typical of these components.

Starting from this background, in this work the erosion resistance of three wear resistant zinc alloys was investigated. In particular, they were studied two standard compositions (ZA27 and Alzen305), well known in literature, and a new ZnAl15Cu1Mg alloy, suitable for both high pressure die casting and forging, that seems to be interesting also for tribological applications [9-10]. Erosion resistance was evaluated via cavitation-erosion tests, according to ASTM G32 standard, using the "stationary specimen" configuration, monitoring the weight loss as a function of test time and analyzing the damaging mechanism. The alloys microstructure and hardness were also assessed in order to find out possible correlations between materials characteristic and erosion resistance. Finally, the eroded areas were examined by scanning electron microscope.

EXPERIMENTAL PROCEDURE

The study was performed on three zinc alloys whose compositions are reported in Tab. 1

ZA27 is characterized by high aluminum content that causes an increase in the mechanical properties and a reduction in castability [11]. It is often used as a substitution of copper alloys, for the production of components that undergo wear also in presence of lubricant [12].

Alzen 305 is a commercial alloy with a little market, developed in the '70ies as a possible substitute for wear resistant copper alloys [13].

ZnAl15Cu1Mg is an innovative alloy, with a lower alloying elements content than the previous alloys, which seems to be very interesting in different fields as a good substitute of both traditional zinc alloys and of some bronzes [3].

Tab. 1 - Chemical composition (wt.%) of the studied alloys
Composizione chimica in peso delle leghe utilizzate

Alloy	Al	Cu	Mg	Zn
ZA27	27	3.5	0.04	rest
Alzen305	44	2.5	0.02	rest
ZnAl15Cu1Mg	15	1	0.04	rest

Figure 1 shows Al-Zn phase diagram and compositions of the studied alloys. All the alloys contain more than 6% of aluminum (eutectic composition), hence the primary phase is rich in aluminum.

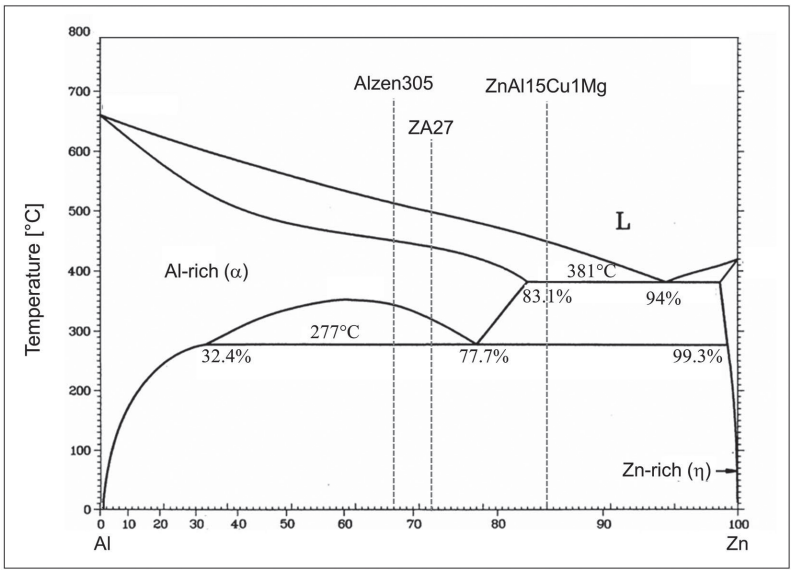

Fig. 1 - Al-Zn phase diagram [14].
Diagramma di stato Al-Zn [14]

The three alloys were obtained by melting certified ingots in alumina crucible, by means of a resistance furnace. The liquid metal was manually poured into steel mold, in order to obtain cylindrical samples with a diameter of 26 mm and a height of 55 mm. Casting temperatures were chosen about 70°C above the liquidus temperature of each alloy, as reported in Tab. 2. Molds were preheated at 220°C.

Tab. 2 - Melting range and casting temperature for the studied alloys
Temperature di liquidus, colata e stampi per le leghe utilizzate

Alloy	Melting range [°C]	Casting Temperature [°C]
ZA27	375-487	550
Alzen305	480-580	650
ZnAl15Cu1Mg	376-435	510

Each sample was cut at 155 mm from the bottom. The two obtained surfaces were polished up to mirror finishing and used for metallographic analyses and cavitation tests respectively.
The microstructure of each alloy was observed via optical microscope (Reichert-Jung MeF3, equipped with Leica QWin software for image analyses), after Nital 2% chemical etching.
Hardness tests were performed by using a micro-hardness tester Shimadzu, with an applied load of 300 g for 15 s. To guarantee a good statistic of the data, at least 30 indentations per sample were done. Only the average values are reported in the text.
Cavitation resistance was evaluated according to ASTM G32 standard, applying the "stationary specimen" method [15]. The ultrasonic apparatus was set to obtain a vibration amplitude of 100 μm and a frequency of 20kHz [16]. The specimens were fixed in a proper holding system to guarantee the positioning of the Inconel® 625 horn tip at 0.5 mm form the samples surface. Both the holding system and horn were placed in a tank filled with demineralized water at constant temperature.
Samples damaging was monitored every hour during the tests, measuring the weight loss of the specimens. Hence, the corresponding volume loss was calculated by considering the density of the alloys, in order to facilitate the comparison between the three compositions.
At the end of the tests, the eroded surfaces were examined with a Scanning Electron Microscope (SEM) LEO EVO 40, in order to study the damaging mechanism.

RESULTS

Alloys microstructure, observed by optical microscope, are reported in Fig. 2.

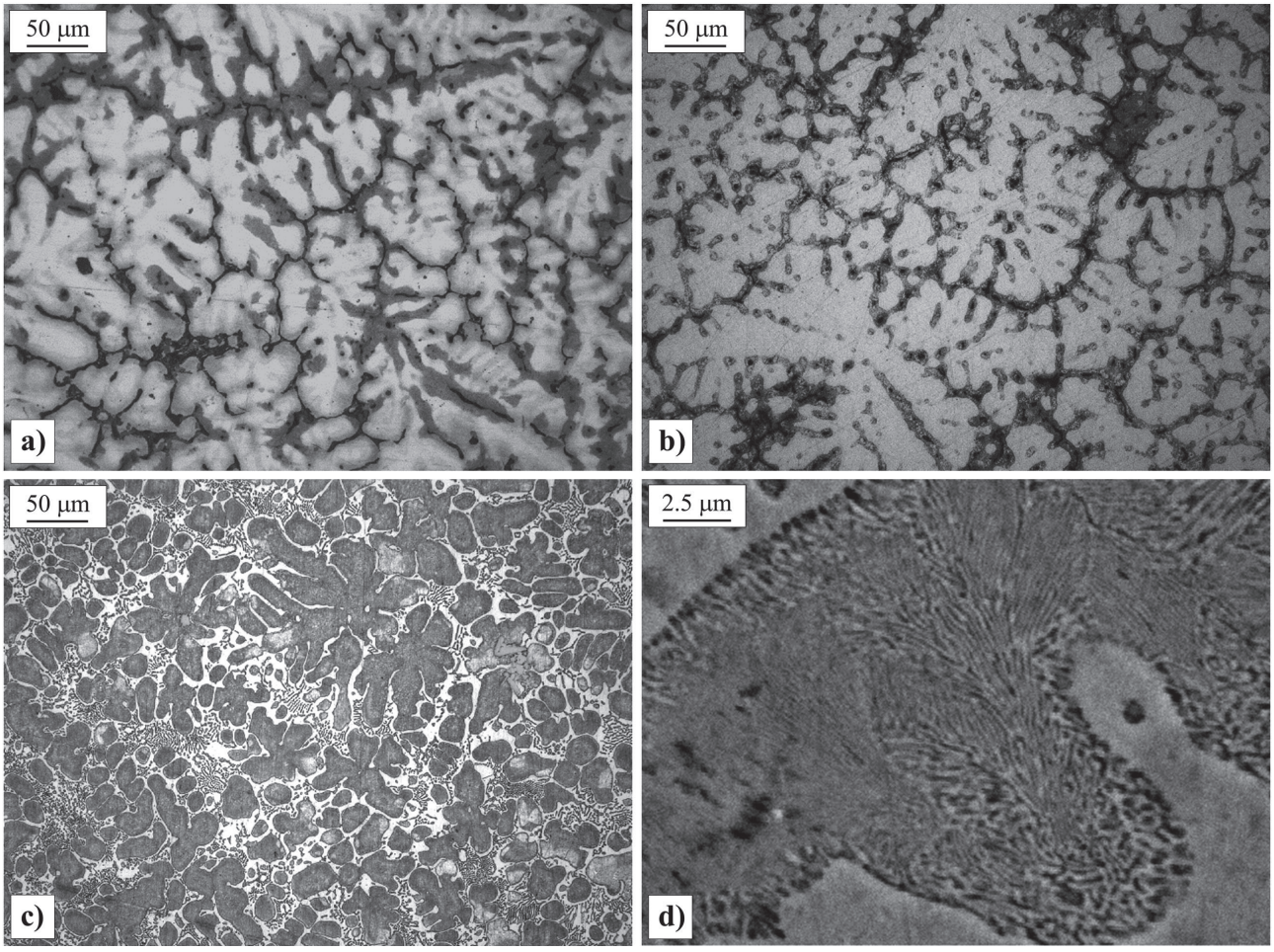

Fig. 2 - Microstructure of the studied alloys: a) ZA27, b) Alzen305, c) ZnAl15Cu1Mg and d) and eutectoid α + η.
Microstruttura delle leghe utilizzate a) ZA27, b) Alzen305, c) ZnAl15Cu1Mg e d) eutettoide α + η.

According to the Al-Zn phase diagram (Fig. 1), the two traditional alloys present only Al-rich β-dendrites with interdendritic films and pools of eutectic [17]. The different colour from the core to the boundary of the arms is due to the different concentration of aluminium, higher in the centre and lower at the borders (Fig. 2a). Differently, ZnAl15Cu1Mg is characterized by primary dendrites of Al-rich β-phase surrounded by the eutectic β+η [18].
During the cooling, all the compositions undergo eutectoid transformation (273°C), that causes the decomposition of the primary β-phase in fine lamellas of α phase (rich in aluminum) and η phase (rich in zinc), visible only by electron microscope at high magnification (Fig. 2d).
The average microhardness values of the three alloys with the respective standard deviations are reported in Table 3. It can be noted that ZnAl15Cu1Mg alloy is softer than the other two traditional alloys, as a consequence of the lower aluminum and copper content [9]. Some authors report the hardness as an indication of the erosion resistance, in particular the higher the hardness, the higher the cavitation resistance [19-20]. Hence, the ZnAl15Cu1Mg can be expected to exploit lower performances than the traditional alloys, due to its lower hardness.

Tab. 3 - HV harness of the studied alloys
Durezza HV delle leghe utilizzate

Alloy	HV hardness	Std. dev.
ZA27	164	5
Alzen305	149	13
ZnAl15Cu1Mg	122	9

On the contrary, this hypothesis is not confirmed by the cavitation tests results, reported in Fig. 3a in terms of volume loss versus time. The eroded volume was calculated from the weight loss measured every hour during the tests, divided by the density values of ZA27 and Alzen305 find in literature (5.0 g/cm^3 [21] and 4.8 g/cm^3 [22] respectively) and calculated by experimental measurements for the new alloy (5.8 g/cm^3). From the graph, it can be seen that the ZA27 is the most damaged alloy, notwithstanding its higher hardness, while Alzen305 and ZnAl15Cu1Mg undergo similar damaging. Analyzing the slope of the linear intercepts, indication of the erosion rate (Fig. 3b), it can be also noted that the erosion rate of the new alloy is lower than that of Alzen305 and ZA27, of 20% and 37% respectively.

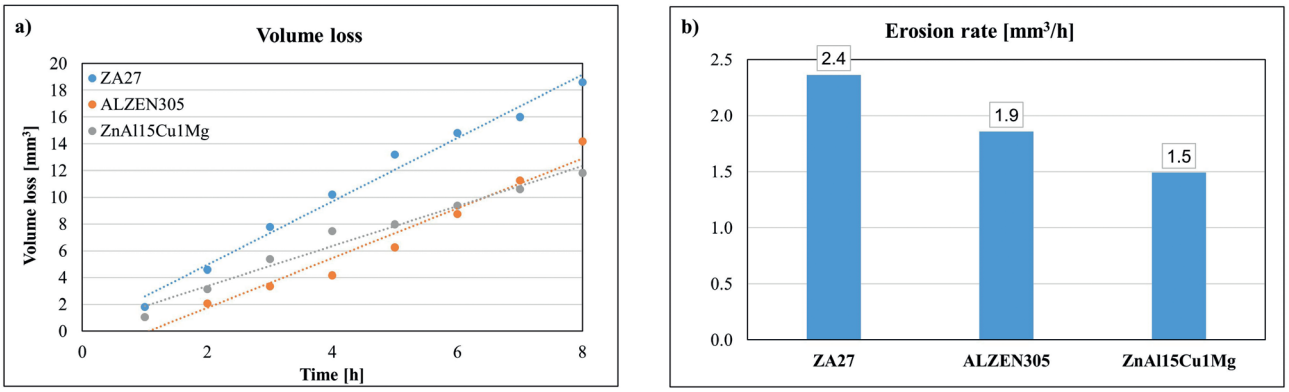

Fig. 3 - Cavitation tests results: a) volume loss vs cavitation time; b) erosion rate
Risultati delle prove di cavitazione: a) perdita di volume in funzione del tempo di trattamento; b) velocità di erosione

The analysis of the eroded areas after 8 hours of test shows an evident and uniform damaging for all the alloys. More in detail, ZA27 surface presents big and deep craters (Fig. 4a), while Alzen305 damaging is mainly related to smaller pits (Fig. 4b). Concerning the ZnAl15Cu1Mg, the eroded surface is more uniform, without evident variation in damaging depth (Fig. 4c).
By increasing the magnification, the exposed surface appears similar for all the alloys, with large areas characterized by high roughness, indicating a damaging mechanism of plastic deformation and subsequent ductile fracture, causing the material dislodgement [23-24].
Some small areas with smooth surface are also present (Fig 4d-f), characterized by fatigue like fracture with striated and flat bottom, caused by the cyclic oscillation of the pressure during the test [23]. These areas were found more frequently on ZA27 and Alzen305 than on the ZnAl15Cu1Mg. Moreover, in ZA27 and Alzen305 samples deep pits are easily detectable (see arrows in Fig. 4a-b), in correspondence of the fatigue-like fractures. These pits cause an increase in the material loss.

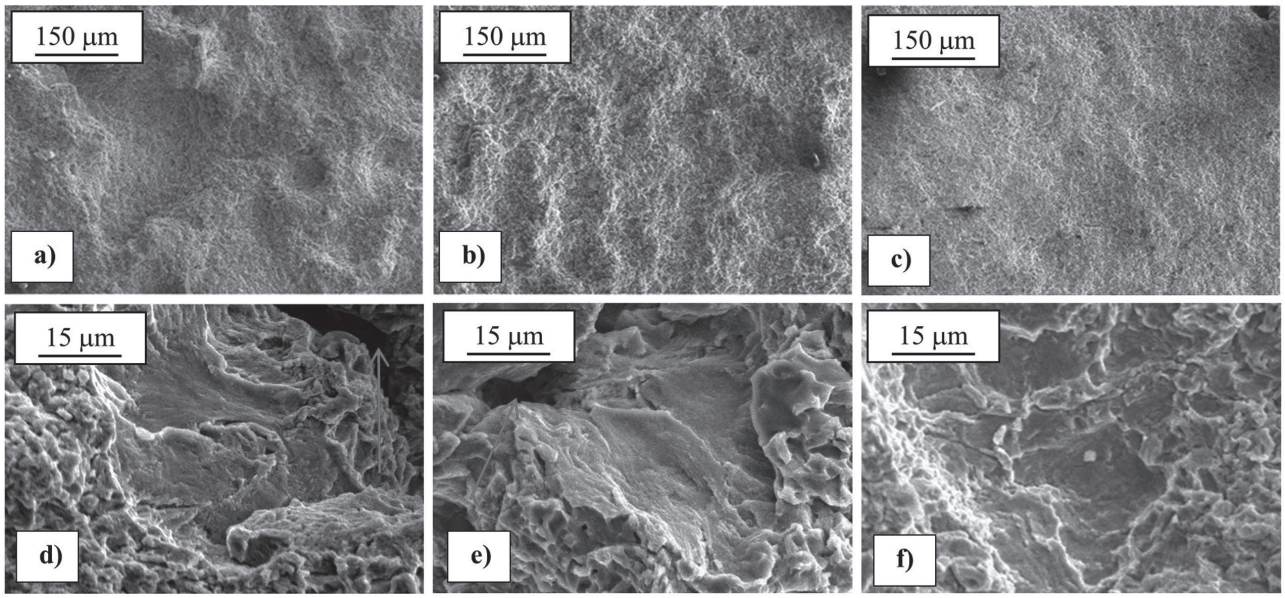

Fig. 4 - SEM analyses of the eroded surfaces after 8 hours: ZA27 (a, d), Alzen305 (b, e) and ZnAl15Cu1Mg (c, f).
Analisi SEM delle superfici erose dopo 8 ore: ZA27 (a, d), Alzen305 (b, e) e ZnAl15Cu1Mg (c, f).

SEM analyses preformed after 8 hours of test do not allow to determine any correlation between microstructure and damaging, as already stated by Hucinska et al. [25] for copper alloys. Hence, to better investigate this aspect, new tests were then carried out taking into account only short exposure times, in the order of 60 s. In the early stages of the cavitation, in fact, it is easier to determine the activation of the erosion mechanism, when only plastic deformation of the surface is present and practically no loss of material is assessable (incubation period) [25].
From the SEM analyses reported in Fig. 5, a relevant damag-

ing of the primary grains can be seen. This is clearly noticeable for ZnAl15Cu1Mg, because after 60 s of test (Fig. 5f) eutectic emerges from the dendrites as visible by comparing the microstructure before (Fig. 5c) and after the test (Fig. 5f).
Based on these findings it can be concluded that the eutectic phase is more resistant then the primary one, in case of the hypereutectic Zn-Al alloy. In the other two alloys, considering the low amount of secondary phases, all the surface appears almost equally damaged. Also for these two compositions the phases at the grain boundaries appear on a higher plane and without any visible damaging.

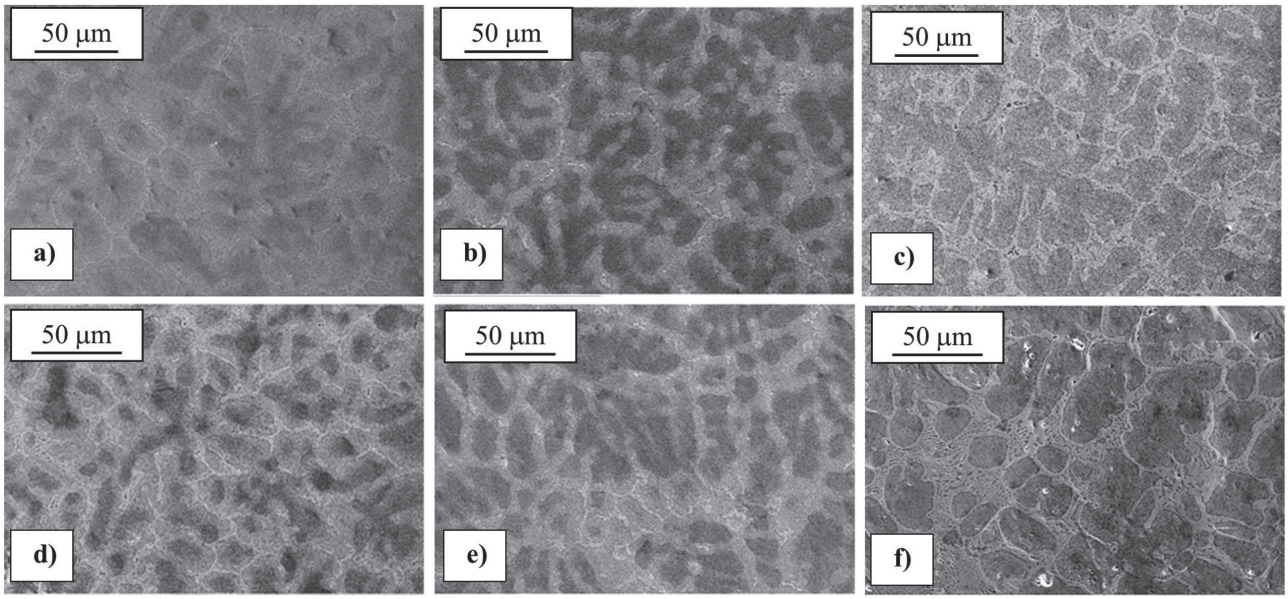

Fig. 5 - SEM analyses of mirror finish surfaces: a) ZA27, b) Alzen305, c) ZnAl15Cu1Mg and after 1 minute of erosion) ZA27, e) Alzen305, f) ZnAl15Cu1Mg.
Analisi SEM delle superfici lucidate a specchio: a) ZA27, b) Alzen305, c) ZnAl15Cu1Mg e dopo 1 minuto di erosione d) ZA27, e) Alzen305, f) ZnAl15Cu1Mg.

To deeply understand and analyse the damaging mechanism for the three alloys, metallographic analyses were carried out on the cross section of the eroded areas (Fig. 6)
Low magnification images (Fig. 6a-c) were collected with the upper edge of the picture coincident with the undamaged samples surface, in order to better discern the magnitude of the damaging depth.
All the alloys show pits or craters. However, the damaging seems more pronounced on the ZA27 whose surface is characterized by deeper and larger pits than the other compositions (Fig. 6a), confirming the SEM analyses performed on the top surface.
Material removal due to the test is related to deep and narrow pits for the Alzen305, while an uniform erosion with shallow pits characterizes the ZnAl15Cu1Mg cross section (Fig. 6c). By increasing the magnification, it is possible to note the presence of cracks (see arrows in Fig. 6a-b), only for the two conventional alloys, starting from the pit bottom and growing in the material along the grain boundaries, that can cause material detachments increasing the weight loss.

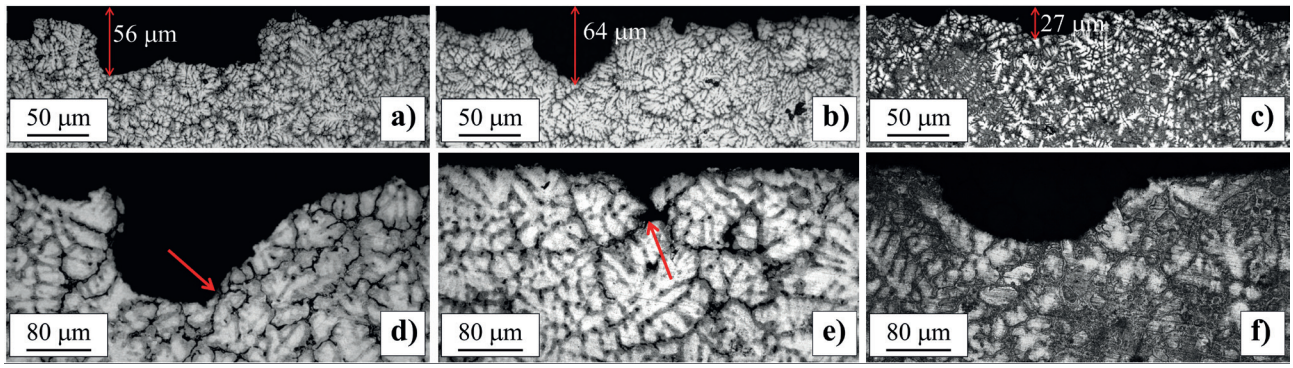

Fig. 6 - Metallography of the eroded surfaces after 8 hours: ZA27 (a, d), Alzen305 (b, e) and ZnAl15Cu1Mg (c, f).
Analisi metallografica delle sezioni erose dopo 8 ore: ZA27 (a, d), Alzen305 (b, e) e ZnAl15Cu1Mg (c, f).

CONCLUSIONI

In this paper the cavitation erosion resistance of a new zinc alloy was analyzed in comparison with two commercial zinc alloys, suitable for bearings production.

It was found that ZA27 and Alzen305 resist less than the ZnAl-15Cu1Mg alloy, notwithstanding their higher hardness. In particular, the erosion rate of the new alloy resulted 20% and 37% lower than that of Alzen305 and ZA27 respectively.

The analysis of the eroded areas after short cavitation time tests showed a damaging mainly located in the primary phase. Hence, in ZA27 and Alzen305 an almost uniform erosion was detected as their microstructure mainly consists in Al-rich β-phase dendrites. On the contrary, in the ZnAl15Cu1Mg, that shows primary dendrites surrounded by the eutectic β+η, the secondary phase appears undamaged, explaining the higher resistance of the new alloy.

Independently from the chemical composition, increasing the cavitation time no correlation between microstructure and damaging mechanism can be determined. The eroded areas of the traditional alloys result characterized by deep craters and pits. Some cracks are also present, nucleating from the bottom of the pits and propagating in the bulk material. Differently, the ZnAl-15Cu1Mg surface appears less rough and smoother.

ACKNOWLEDGMENTS

Authors thanks D. Rollez from Grillo-Werke AG, for the materials supply, and D. Paderno for the holding system design and realization.

REFERENCES

[1] M.D. Hanna, J.T. Carter, M.S. Kashid, Wear 203-209 (1997) 11-21.
[2] M.T. Abou El-Khair, A. Daoud, A. Ismail, Mater. Lett. 58 (2004) 1754-1760.
[3] A. Pola, L. Montesano, M. Gelfi, G. M La Vecchia, Wear 368-369 (2016) 444-452.
[4] G. Pürçek, T. Savaşkan, T. Küçükömeroğlu, S. Murphy, Wear 252-11-12 (2002) 894-901.
[5] S. Yan, J. Xie, Z. Liu, W. Wang, A. Wang, J. Li, J. Mater. Sci. Technol. 26-7 (2010) 648-652.
[6] D. Apelian, M. Paliwal, D.C. Herrschaft, JOM (1981) 12-20.
[7] D. Rollez, A. Pola, F. Prenger, World of Metallurgy - Erzmetall 68-6 (2015) 354-358.
[8] B.K. Prasad, A.K. Patwardhan, A.H. Yegneswaran, Wear 199 (1996) 142-151.
[9] A. Pola, G. M La Vecchia, M. Gelfi, L. Montesano, Metall. Ital. 4 (2015) 37-41.
[10] T. Savaşkan, A. P. Hekimoğlu, Int. J. Mater. Res. 107- 7 (2016) 646-652.
[11] E. J. Kubel, Expanding horizons for ZA alloys, Adv. Mat. Proc. (1987) 51-57.
[12] K.J. Altorfer, Metal Prog.122-6 (1982) 29-31.
[13] P.P. Lee, T. Savasakan, E. Laufer, Wear 117 (1987) 79-89.
[14] ASM Handbook – Vol. 3: Alloy phase Diagram, ASM international, Materials Park, Ohio (1992).
[15] ASTM G 32 standard. Standard Test Method for Cavitation Erosion Using Vibratory Apparatus.
[16] A. Arrighini, M. Gelfi, A. Pola and R. Roberti, Mater. Corros. 61-3 (2010) 218-221.
[17] M. Durman, S. Murphy, J. Mater. Sci. 32 (1997) 1603-1611.
[18] T. Savaşkan, A. P. Hekimoğlu, Mat. Sci. Eng. A-Struct. 603 (2014) 52-57.
[19] S. Vaidya, C. M. Preece, Metall. Trans. A 9A (1978) 299-307.
[20] A. Karimi, J.L. Martin, Int. Mater. Rev. 31-1 (1986) 1-26.
[21] K. Chakrabarti, Casting technology and cast alloys, Prentice, Hann of India, New Dely (2005).
[22] L. L. Shreir, Corrosion: Metal/Environment Reactions, Newnes-Butterworths, London (1976).
[23] W. J. Tomlinson, S. J. Matthews, J. Mater. Sci. 29-4 (1994) 1101-1108.
[24] B. Vyas, C.M. Preece Met. Trans. A 8 (1977) 915-923.
[25] J. Hucińska, M. Glowacka, Metall. Mater. Trans. A 32-6 (2001) 1325-1333.